Distributed Control of Converters in Parallel with Load Sharing

Isabel Gallego Tavares
isabel.gallego@tecnico.ulisboa.pt

Instituto Superior Técnico, Lisboa, Portugal

November 2022

Abstract

This work presents the study of the topology and control of a DC-DC converter for further study of the connection in parallel with other modules with the existence of load sharing between them.

The converter used is of the buck type that has an input voltage of 100V. This converter presents a voltage value at its output lower than that of the power supply through the pulse width modulation technique, applied to a power MOSFET as a switching element. The converter operates at a frequency of 50kHz and has an output voltage of 48V. The output voltage remains constant and equal to the reference voltage that is initially defined and introduced in the *software* used to carry out the simulations, even if there are variations in the current required by the load. The converter control is initially done using two loops with feedback and PI controllers, an internal one for current control and an external one for voltage control. Then resistive and inductive virtual inductances are implemented. Then, two converters are connected in parallel, applying the different control techniques to all of them.

Finally, results from simulations are presented in order to compare the different control methods applied.

Keywords: Buck Converter, Microgrids, PI Control, PWM, Virtual Impedance.

1. Introduction

Emissions of carbon dioxide (CO2) and consequent damage to the ozone layer, global waMGing, among others, have boosted the use of safe, renewable, ecological, clean and green energy sources.

In recent decades, there has been a continuous increase in the consumption of renewable energies, such as photovoltaic and wind, due to many advantages, namely:

- low dependence on biomass;
- decrease in CO2;
- fuel price.

Green energies also brought the concept of controllable, interactive and independent Microgrid (MR).

A MG consists of the interconnection of different distributed energy sources, such as wind turbines, photovoltaic panels, different loads, electric vehicle charging stations, control and communication system for sharing energy within the MG or other networks, as well as energy storage.

MGs can usually operate in two modes: connected to the grid, or disconnected from the grid, that is, in island mode. It is also possible to classify them as Direct Current (DC), Alternating Current (AC) or hybrid MGs, depending on the type of bus to which the power electronic interfaces are connected.

There are several advantages over paralleling DC-DC converters, including greater reliability and greater efficiency [1]. In distributed power systems, parallel-connected converters have been used for many years [2]. The main problem faced by DC MR is that when the converters are connected in parallel, the converter output voltage will not always be constant [3],[4]. The main reason for this variation is due to load variations, input power and also the feedback voltage and current [5],[6].

The interconnection of distributed generators to the grid through electronic power converters raises concerns about the stability of the system and the smooth transition between grid-connected and island modes. Many innovative control techniques have been used both for system stability and for proper load sharing, with the most common method for controlling this load sharing being the *droop* control method.

The stability of the system during load sharing has been explored by many researchers, namely in [7],[8].

2. Converter

The DC-DC converters allow the conversion of a continuous value of voltage or current to another

value of different amplitude but also continuous.

In general, these converters are made up of high frequency switched semiconductors and passive components such as capacitors and coils. These converters are controlled through a PWM signal, the duty cycle being the main characteristic that controls the voltage value at the circuit output.

As there are several topologies of DC-DC converters, it is possible to obtain a wide range of topologies, each one with its degree of specificity and complexity. It is possible to classify them into two distinct groups: isolated and non-isolated. The difference between these two depends mainly on the existence of galvanic isolation between the power supply and the circuit output, that is, on the use of a high frequency transformer in isolated converters.

In addition to the distinction made, we can also classify the converters according to their purpose.

The converter chosen for the development of this work was the voltage reduction converter, since it is intended to obtain an output voltage lower than the voltage imposed on the input.

One of the design options that must be taken into account when dimensioning converters is the choice of the type of controlled semiconductor to be used, depending on the specific application in which it is inserted. In this way, for your choice it is usual to take into account several factors, such as:

- device cost;
- voltage and current limit values;
- complexity of command and trigger circuits;
- frequency at which it will operate.

Thus, in view of the project under analysis, we chose to use a MOSFET type semiconductor (metal-oxide-semiconductor field effect transistor) and the model chosen was the G3R60MT07K 750V 60 mΩ SiC from the manufacturer GeneSiC . It is a MOSFET capable of supporting 750V at its terminals and the maximum supported current value is 26A.

3. Converter Control

3.1. Proportional Integral Control

Proportional Integral (PI) control is a closed-loop control mechanism that continuously calculates the error value between the difference of a reference value and a process variable to be controlled, applying the necessary correction in proportional terms. and integrals. Both implementation and scaling are relatively simple [9]. The proportional term makes a change in the output that is proportional to the current error value. Thus, the controller output signal is always multiplied by the error, which leads to a non-zero value error, its value being inversely proportional to the gain K_p, which can be compensated by means of integral control. If the proportional gain is too high, the output value will be too, which can lead to system instability. On the contrary, if this gain is too low, the system may not take the necessary action to correct the disturbance.

The contribution of the integral part aims to eliminate the error in steady state. An output signal proportional to the amplitude and duration of the error is produced, which provides an alternative to correct the non-zero error generated by the proportional action, while accelerating the response of the system, causing it to reach the value more quickly. of reference.

Figure 1 shows the architecture of a PI controller.

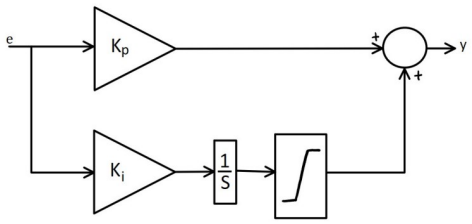

Figure 1: Block diagram of a PI controller

The equation that describes it is given by

$$C(s) = K_p + \frac{K_i}{s} \tag{1}$$

where the parameters K_i and K_p represent the integral and proportional gains, respectively, and their expressions are deduced through the closed-loop transfer function.

These controllers can either be implemented in an analog way, using operational amplifiers, or in a digital way, using microcontrollers.

The control developed in this article involves the application of this type of control to both current and voltage. Thus, it is necessary to dimension the parameters for each of these cases.

Starting with the current, the objective is to set I_L equal to the value defined as reference (I_{Lref}). Through the equations 2 and 3, we can obtain the values of the integral and proportional gain, respectively.

$$K_i^i = \frac{1}{T_p} = \frac{1}{4\xi^2 k_i K_m \frac{T}{2R}} \tag{2}$$

$$K_p^i = \frac{T_z}{T_p} = \frac{L}{4\xi^2 k_i K_m C \frac{T}{2R}} \tag{3}$$

As far as voltage is concerned, the scaling is very similar. Its parameters are calculated using the equations 4 and 5.

$$K_i^u = \frac{1}{T_p} = \frac{1}{8\xi^2 K_c R \alpha \frac{T}{2}} \tag{4}$$

$$K_p^u = \frac{T_z}{T_p} = \frac{C}{8\xi^2 K_c \alpha \frac{T}{2}} \quad (5)$$

Throughout this work, the value of ξ is fixed at $\frac{\sqrt{2}}{2}$. This value usually results in a response with a faster settling time and a reasonable *overshoot* [10].

3.2. Virtual Impedance

The main objective of control based on a virtual impedance is to improve the dynamic response of DC MRs under varying loads. It also serves to ensure better load distribution across the various converters.

In order to complete the current and voltage control loop developed using PI control, a virtual impedance loop was also implemented for energy management. In order to test different possible scenarios, this virtual impedance loop was equipped with resistive, inductive and capacitive impedance. In the following subsections, the implemented methods will be described.

3.2.1 *Droop* Control

The method by *droop* control, also known as virtual resistance, was first introduced for sharing current between voltage-regulated modules connected in parallel [11], as shown in the figure 2.

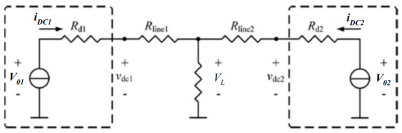

Figure 2: Simplified equivalent circuit of two DC sources in parallel feeding a common load bus

There are different *droop* control strategies, which can be grouped into two distinct groups - voltage-mode and current/power-mode control. In the first group, the current is measured and fed to the control, while in the second group, the control is fed by the measured output voltage [12].

- *droop* control by voltage mode:
  - Voltage - current: the output current is measured and fed to the control;
  - Voltage - power: the output power is measured and fed to the control.
- Control *droop* by current/power mode:
  - Current - voltage: the output voltage is measured and fed to the control;
  - Power - voltage: the output voltage is measured and fed to the control.

As voltage mode control will be used in this work, namely voltage - current, this method will only be described in greater detail.

For its implementation, the equations 6 and 7 [12] were followed, which translate into the block diagram represented in the figure 3.

$$V_{DC} = V_{0max} - R_D(i_{DC} - I_{0min}) \quad (6)$$

$$R_d = \frac{V_{0max} - V_{0min}}{I_{0max} - I_{0min}} \quad (7)$$

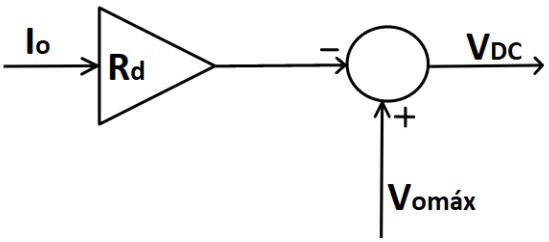

Figure 3: Block diagram of *droop* control by voltage mode (voltage-current)

The application of this control technique increases the accuracy of current sharing and helps in regulating the voltage on each load that is connected to the converter. As illustrated in the figure 2, two DC voltage sources were connected to different loads in series with the resistance of *droop*, the loads being connected in parallel.

The voltage-current characteristics of the equivalent circuit (shown in the figure 4) show that for small values of *droop* resistance, the voltage regulation at each load is smaller and the current error ($i_2 - i_1$) is larger. On the contrary, when the value of this resistance is higher, the voltage regulation at each load is also higher and the current error is lower. In this way, it can be seen that a moderate value of drop resistance both maintains voltage regulation and keeps the error of the output current in the limit. The drop resistance is chosen so that there is a compensation between voltage regulation and current distribution.

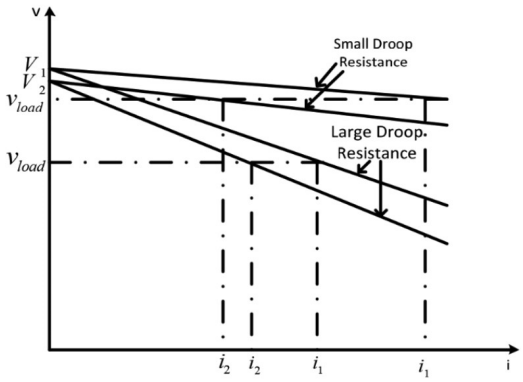

Figure 4: Equivalent circuit voltage-current characteristics

The figure 5 shows the block diagram of the proposed strategy applied to two converters connected in parallel. The control scheme consists of two internal current and voltage control loops and an external control loop via virtual impedance.

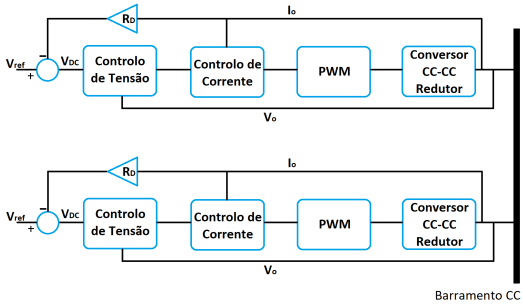

Figure 5: Control scheme of DC-DC converters in parallel using the virtual resistive impedance method

For higher output currents, this method is not as effective but it is notable for achieving good voltage regulation on the load of each converter.

This centralized control technique was the first step towards current sharing in MG DC.

3.2.2 Impedância Indutiva

Following the basis of *droop* control, a virtual inductance was considered in order to improve the transient response of the control unit. In place of the *droop* resistor, a Low Pass Filter (FBP) is placed, in order to minimize noise and its output goes to the virtual inductive impedance (L_D) [13].

The derivative block diagram of this control strategy is illustrated in figure 6.

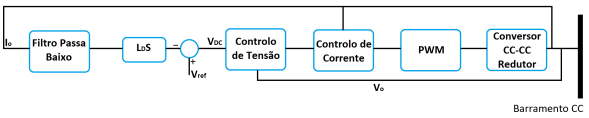

Figure 6: Control scheme of DC-DC converters in parallel using the virtual inductive impedance method

The value of L_D is given by the inverse of the integral voltage gain [14]:

$$L_D = \frac{1}{K_i^u} \tag{8}$$

The FPB transfer function is governed by the following equation:

$$F = \frac{1}{Ts + 1} \tag{9}$$

where the filter coefficient (T_f) is given by the fraction between the proportional voltage gain and the integral voltage gain:

$$T_f = \frac{K_p^u}{K_i^u} \tag{10}$$

K_i^u and K_p^u are calculated using the equations 4 and 5, respectively. The resulting value of this loop (V_{DC}) is used as one of the inputs for the voltage control, in order to be able to calculate the error between this same value and the reference value.

4. Simulation and Results

4.1. Control of two converters

It is intended to use more than one converter and all of them connected in parallel. Thus, simulations were performed for two converters connected in parallel. The developed model is represented in the figure 7.

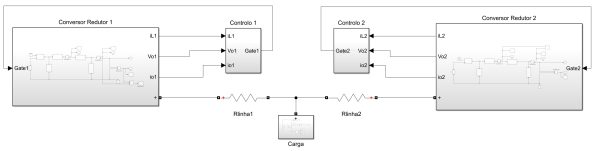

Figure 7: Diagram of two step-down converters connected in parallel

The subsystems *Conversor Redutor 1* and *onversor Redutor 2* represent the developed converters (figure 8). The resistors R_{line1} and R_{line2} correspond to the line resistors of the first and second converters, having been assigned a value of 0.1Ω and 0.01Ω, respectively. The subsystem called load, which includes the load resistance fed by the two converters in parallel, can be seen in greater detail in the figure 9.

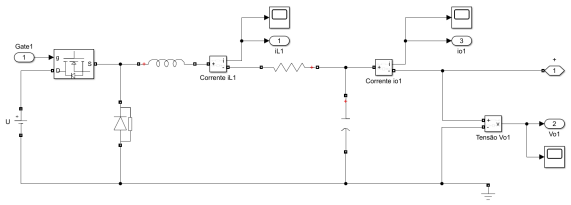

Figure 8: Schematic of the buck converter used

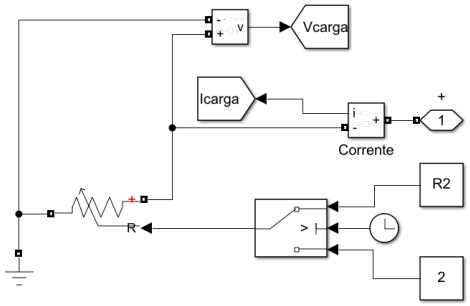

Figure 9: Schematic of the load supplied by the two converters

The parameters of the Buck Converter 1 and 2 can be consulted in the table 1.

Table 1: Parameters used in the simulation of Buck Converters 1 and 2

	Converter	
	1	**2**
P	1500W	1000W
I_L	31.25A	20.83A
L	0.1597mH	& 0.24mH
Δi_L	3.125A	2.083A
C	16.28μF	10.9μF
Δv_o	0.48V	0.48V

In the following sections, two different control techniques applied to these two converters connected in parallel will be studied. These systems first consist of applying the *droop* method to both converters and simulating both converters controlled through the system with virtual inductance.

4.1.1 Application of *droop* method in both converters

Initially, the control system explained in 3.2.1 was implemented in both converters.

In the table 2, the values of the parameters used to control both drives using this system can be viewed. For the maximum and minimum voltage values (V_{0max} and V_{0min}) a margin of plus or minus 5% was given over the output voltage value, respectively. Regarding the current, for its minimum value it was considered that it was 20% of the maximum value, which was defined as 40A.

Table 2: Control parameters of the two drives for the control system with application of the *droop* method on both drives

Parameter	**Converter 1**	**Converter 2**
I_{0max}	40A	25A
I_{0min}	8A	5A
V_{0max}	50.4V	50.4V
V_{0min}	45.6V	45.6V
R_d	0.15Ω	0.24Ω

The gains for the respective PI controllers of both converters can be consulted in the table 3.

Table 3: Values of the proportional and integral gains used in the double-loop control of the Buck Converter 2

	Converter	
	1	**2**
K_i^i	768	1152
K_p^i	0.0799	0.1198
K_i^u	1.6276×10^4	1.0851×10^4
K_p^u	0.4069	0.2713

Analyzing the figure 10 (a) which shows the waveforms of i_{o1}, in red, and i_{o2}, in blue , referring to the first and second converters, respectively, it is possible to observe that before the load changes its value, i_{o1} has an average value of 14.9A and i_{o2} a value of 8.5A. From the moment the system changes the load value and it stabilizes, these variables present an average value of 13.1A and 7.4A, in that order. This difference in values between currents is natural, since the converters have different power supply. That is, for the converter with a higher power, the current will naturally be higher and, for a lower power, the current will also be lower.

As for the output voltage waveforms represented in 10 (b), it should be noted that both stabilize in the desired range of values (between V_{0max} and V_{0min}), either before the load change or after. At the moment when this variation occurs, the voltage in both converters reaches a peak, but even this is within acceptable values.

At 20ms there is a load variation, causing the average current value to decrease and, therefore, the voltage value to rise slightly.

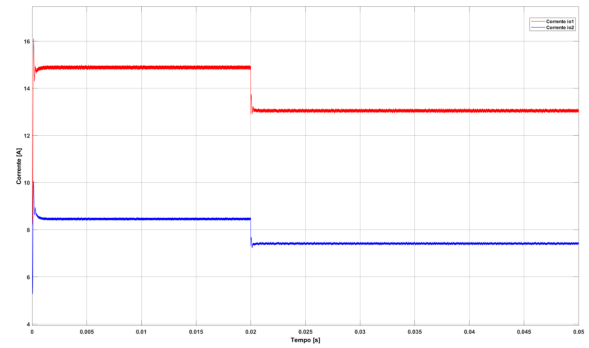

(a) Corrente de saída i_{o1} (vermelho) e i_{o2} (azul)

(a) Output current i_{o1} (red) and i_{o2} (blue)

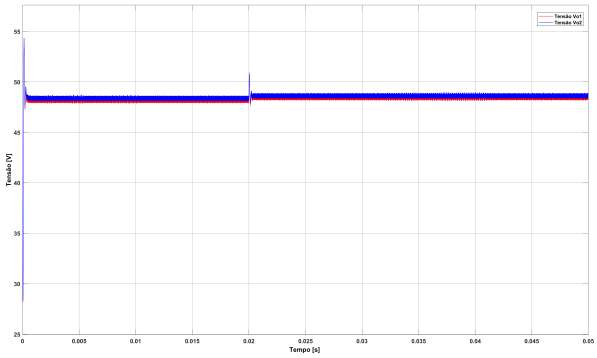

(b) Output voltage V_{o1} (red) and V_{o2} (blue)

Figure 10: Waveforms of (a) i_o and (b) V_o resulting from the control system with application of the *droop* method in both converters

In general, we can conclude that this control system works when you want to control two converters in parallel.

4.1.2 Application of the virtual inductance method in both converters

In this subsection, the control system with the application of virtual inductive impedance in both converters will be described. Using the equation 8 again, it was possible to calculate the parameter L_{D1} used in the control of the Buck Converter 1.

$$L_{D1} = 61.440\mu H$$

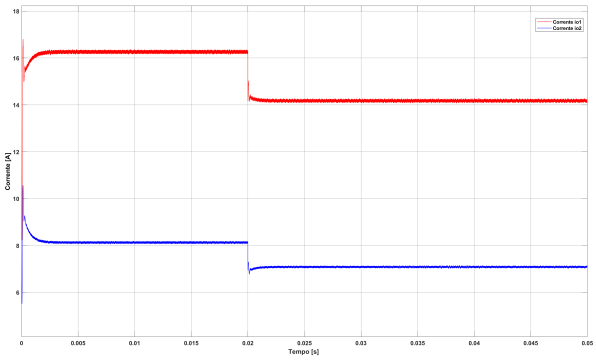

(a) Output current i_{o1} (red) and i_{o2} (blue)

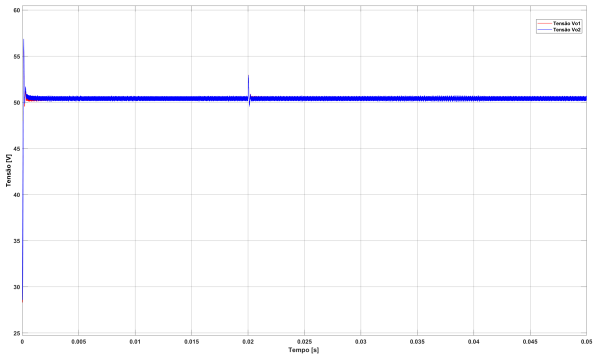

(b) Output voltage V_{o1} (red) and V_{o2} (blue)

Figure 11: Waveforms of (a) i_o and (b) V_o resulting from the control system with application of the virtual inductance method in both converters

Regarding the output currents of each converter, we have again that i_{o1} is higher than i_{o2} at all times of the simulation. Compared to other systems, i_{o1} now has the highest values while i_{o2} has the lowest values.

Examining the waveforms of V_{o1} and V_{o2} over time, it is clear that they overlap when they stabilize, even though there is a transition of powered load. With this control system both output voltages have an average value of 50.4V, the exact value for which they are being controlled. Thus, we can say that even when the load value varies, the system always manages to converge to the desired reference value, demonstrating robustness with regard to load variation.

With the application of this system, i_o and V_o continue to take relatively longer to reach a constant value at both times compared to the point control system 4.1.1.

5. Conclusions

The article developed has as main objective to design a prototype of an electronic converter capable of feeding a direct current bus in which the output voltage can follow a certain reference voltage, which is initially defined. The output voltage must remain constant and equal to this reference voltage even if there are variations in load values.

With the accomplishment of the present work, it was possible to evaluate different solutions for the implementation of control systems in DC-DC Buck Converters, highlighting, for the control of two converters connected in parallel, the point system 4.1.2, which consists of the use of virtual inductive impedance in both converters. The implemented block diagram can be consulted in the figure 6. This system was found to be more efficient as it always maintains the same V_{load} throughout the simulation time, even when there is variation in the shared load, with the exception of transient moments. The other control system developed for the connection of two converters proved to be more sensitive to these variations and, therefore, is not as effective for the intended purpose, despite being able to maintain the desired voltage.

Thus, with regard to the control of inverters in parallel with shared load, it is possible to conclude that the implementation of control systems equipped with inductive virtual impedances are more efficient than systems controlled by the *droop* method.

Acknowledgment

This work is the culmination of an academic training course at Instituto Superior Técnico in which several people, directly or indirectly, played an important role. To all of them, my thanks.

However, I would like to give a special thanks to the people who are closest to me, since they were the most sacrificed for the same.

As such, I want to thank my mother Carla Alvarez and my brother Artur Tavares for the love, affection, patience, support, education and strength that any student needs and should have throughout their academic journey.

Availability and support was always needed.

In the same way, we thank the friends with whom we developed bonds and emotions throughout this course, and to whom I also owe part of its accomplishment.

To everyone else, who made this journey but who are not obliged here, my very much!

References

[1] H. Iu and C. Tse. Study of low-frequency bifurcation phenomena of a parallel-connected boost converter system via simple averaged models. *IEEE Transactions on Circuits and Systems*, 50(5):679–686, May 2003.

[2] K. Rinne, A. Kelly, and E. O'Malley. A novel digital single-wire quasi-democratic stress share scheme for paralleled switching converters. *Powervation Ltd., Limerick, Ireland*, 2010.

[3] C. Hua and C. Shen. Study of maximum power tracking techniques and control of dc/dc converters for photovoltaic power system. pages 86–93, 1998.

[4] H. Huang, C. Hsieh, J. Liao, and K. Chen. Adaptive droop resistance technique for adaptive voltage positioning in boost dc–dc converters. *IEEE Trans. Power Electron*, 26(7):1920–1932, Jul. 2011.

[5] S. Anand, B. G. Fernandes, and M. Guerrero. Distributed control to ensure proportional load sharing and improve voltage regulation in low voltage dc microgrids. *IEEE Trans. Power Electron*, 28(4):1900–1913, Apr. 2013.

[6] S. Anand and B. Fernandes. Modified droop controller for paralleling of dc-dc converters in standalone dc system. *Power Electronics, IET*, 5(6):782–789, Jul. 2012.

[7] M. C. Chandorkar, D. M. Divan, and R. Adapa. Control of parallel connected inverters in standalone ac supply systems. *IEEE Transactions on Industry Applications*, 29(1):136–143, 1993.

[8] M. Reza, D. Sudarmadi, F. A. Viawan, W. L. Kling, and L. Van Der Sluis. Dynamic stability of power systems with power electronic interfaced dg. *Power Systems Conference and Exposition, PSCE'06*, pages 1423–1428, 2006.

[9] R. G. Kanojiya and P. M. Meshram. Optimal tuning of pi controller for speed control of dc motor drive using particle swarm optimization, *IEEE*. page 6, 2012.

[10] Setting the p-i controller parameters, kp and ki, application-note tle7242g and tle8242. Infineon Technologies AG, Oct 2009.

[11] Y. Ito, Y. Zhongqing, and H. Akagi. Dc microgrid based distribution powergeneration system. *The 4th Int. Power Electronics and Motion Control Conf.,Xi'an, China*, 2004.

[12] Dc microgrids – droop strategies. Technical report, Instituto Superior Técnico, 2020.

[13] M. Hamzeh, M. Ashourloo, and K.Sheshyekani. Dynamic performance improvement of dc microgrids using virtual inductive impedance loop. *The 5th Power Electronics, Drive Systems and Technologies Conference*, Feb. 2014.

[14] Z. Cheng, M. Gong, J. Gao, Z. Li, and J. Si. Research on virtual inductive control strategy for direct current microgrid with constant power loads. *Applied Sciences*, Oct. 2019.